Evidence of deep traps in overgrown v-shaped defects in epitaxial GaN layers

P. H. Weidlich,[1] M. Schnedler,[1] H. Eisele,[2] U. Strauß,[3] R. E. Dunin-Borkowski,[1] and Ph. Ebert[1,a)]
[1]*Peter Grünberg Institut, Forschungszentrum Jülich GmbH, 52425 Jülich, Germany*
[2]*Institut für Festkörperphysik, Technische Universität Berlin, Hardenbergstr. 36, 10623 Berlin, Germany*
[3]*OSRAM Opto-Semiconductors GmbH, Leibnizstr. 4, 93055 Regensburg, Germany*

(Received 24 June 2013; accepted 15 July 2013; published online 5 August 2013)

The geometric and electronic structure of overgrown v-shaped defects in GaN epitaxial layers are investigated by cross-sectional scanning tunneling microscopy and spectroscopy. The v-defects are found to be hexagonal pit structures delimited by six $\{11\bar{2}2\}$ planes. The electronic properties are inhomogeneous. In some areas the center of the v-defects exhibits a strongly inhibited tunneling current, indicating the presence of deep traps. © *2013 AIP Publishing LLC*.
[http://dx.doi.org/10.1063/1.4816969]

Group III-nitride semiconductors are well known to exhibit excellent optoelectronic properties within the spectral range from ultraviolet to green. Hence they are the material system of choice for highly efficient light emitters.[1] However, the main drawback of group III-nitride semiconductors is the lack of large bulk material substrates for the growth of optoelectronic devices. Therefore, most epitaxial layers have to be deposited on lattice-mismatched and thermal-mismatched substrates or on pseudo substrates. In both cases, the defect density is rather high, influencing the optoelectronic properties of the epitaxial layers.

The most prominent defects during growth of epitaxial layers of group III-nitride semiconductors are—besides dislocations—the so called v-shaped defects or inverted pyramidal pits, occurring on the growth surface typically around threading dislocations.[2–5] These v-shaped pits can reach very high concentrations. However, at present it is unclear how the v-shaped pits at the growth front will affect the resulting epitaxial material once they are overgrown.

Unfortunately, the cross-sectional investigation of overgrown v-shaped defects in pure group III–nitride semiconductor layers is a difficult task. Hence, the information on overgrown v-shaped defects in pure GaN is limited. In transmission electron microscopy only v-shaped defects in multiple quantum wells formed by different group III-N alloys yield a strong contrast and were thus far investigated,[2,6–14] focusing on the geometric structure of the v-shaped defects and the presence of further defects therein. However, in these cases the electronic structure may be modified by the presence of quantum wells.

The sparse electrical characterization of v-shaped defects in pure GaN shows strongly broadened cathodoluminescence spectra on both the growth surface[15] and at overgrown v-defects.[16] This indicates a locally increased free electron concentration of the v-shaped defects[15,16] or at least an optically different zone extending along the *c*-(growth) direction.[17] In addition, there are indications that the concentration of oxygen impurities increases[2,18] in the v-shaped defects, which may act as donors. Top-view measurements show an increase in the work function and the leakage current at v-pits on *n*-type GaN.[19] In contrast, other experiments suggest that the v-defects are recombination centers[5,20,21] or suggest that the minority carrier lifetime is longer inside v-defects.[22] However, it is unclear to what degree these results are affected by the pinning of the Fermi energy at the polar *c*-plane surface.[21] Hence, the electronic structure of *overgrown* v-shaped defects in pure GaN remains unclear.

Here we investigate overgrown v-shaped defects in GaN epitaxial layers by cross-sectional scanning tunneling microscopy (XSTM) and spectroscopy. We identify the geometrical structure and illustrate inhomogeneous electronic properties with evidence of deep traps locally inhibiting electron tunneling.

In order to visualize overgrown v-shaped defects in XSTM images, we utilize an *n*-type doping modulation along the *c*-(growth) direction within the epitaxial GaN layers. Such a doping modulation is easily visible in XSTM images due to the induced slight potential modulation.[23] The modulation visualizes the shape of the growth front after overgrowth. The samples were cleaved in ultrahigh vacuum (1×10^8 Pa) along a *m*-$(10\bar{1}0)$ plane, opening a cross-sectional view on the epitaxial layers.[24] For the XSTM measurements we used electro-chemically etched tungsten tips.

A constant-current XSTM image of a typical v-shaped defect exposed at a cross-sectional GaN$(10\bar{1}0)$ cleavage surface is shown in Fig. 1. The [0001] growth direction is toward the right side of the image. The cleavage surface exhibits terraces separated by steps. Some of these steps abruptly terminate at dislocation lines intersecting the cleavage surface (see circles in Fig. 1).[25] Superimposed on the stepped surface, a roughly periodical contrast change arising from a doping modulation can be discerned as dark contrast lines. The modulation contrast is marked by arrows above and below the XSTM image. The orientation of the doping modulation exhibits a sharp v-shape in the center of the image (see (yellow) dashed line in Fig. 1). The v-shaped edges are propagating along growth direction over several tens of micrometers, reaching ultimately the final growth

a)Electronic mail: p.ebert@fz-juelich.de

 © 2013 AIP Publishing LLC

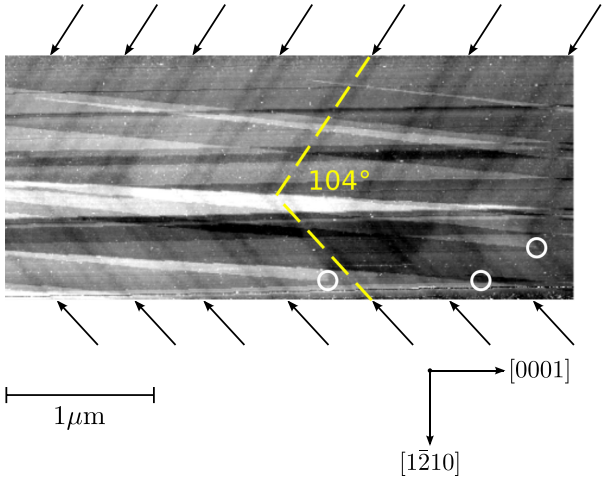

FIG. 1. Constant-current XSTM image of a cleaved (10$\bar{1}$0) surface of a modulation doped GaN epitaxial layer showing a cross-section through a v-shaped defect. The arrows below and above the XSTM image indicate the doping modulation. The v-shaped structure is indicated by the (yellow) dashed line. The surface exhibits many cleavage steps running preferentially horizontally and forming narrow triangular terraces, superimposed on the contrast of the doping modulation. The circles mark dislocation lines intersecting the cleavage surface. The image shows the empty density of states acquired at a voltage of +4.0 V and 100 pA of set current.

surface. It should be noted that the doping modulation essentially traces the original growth front. Hence the observed v-shaped edge in the modulation is indicative of an overgrown v-shaped defect at the growth surface.

Figure 1 illustrates that the v-shaped defects opens toward the [0001] direction. The main structural property of the v-defect is its opening angle. In order to measure this angle in the STM image, we corrected the nonlinear distortion of the XSTM image arising from the properties of the scanning tube using a calibration sample with periodic TiO_2 dots.[26] The correction allows to determine the average angle of all observed v-shaped defects to be $104° \pm 5°$. The wurtzite structure consists of three equivalent $\{10\bar{1}0\}$ (m-) planes, which all can be cleaved. Hence, we cleaved the samples on the three 60° rotated $\{10\bar{1}0\}$ surfaces to extract the geometrical structure of the v-defect in all three dimensions. On all cleavage surfaces, we observed the same opening angle within the accuracy of the measurement. Thus the overgrown v-shaped defect is a 1-dimensional defect orientated along the growth direction with an inverted pyramidal structure at the growth surface.

In previous investigations inverted hexagonal or dodecagonal pyramids were found having $\{10\bar{1}1\}$ (Refs. 2–10, 12, 13, 15–18, 21, and 22) or $\{11\bar{2}2\}$ (Ref. 27) facets, or both,[11,28] depending on the growth conditions. In order to determine which type of these semi-polar facets occurs in the sample here, we turn to the structural models of inverted hexagonal pyramids consisting of only $\{11\bar{2}l\}$ or only $\{10\bar{1}k\}$ $(k, l > 0)$ planes (Fig. 2). An inverted hexagonal pyramid consisting of $\{11\bar{2}l\}$ facets exhibits a v-shape in an m-plane cross section (Fig. 2(c)), whereas pyramids consisting of $\{10\bar{1}k\}$ planes have a cross section with a flat bottom in the m-plane (Fig. 2(f)). In the investigated samples, we never observed a cross-section of a v-shape with flat bottom.

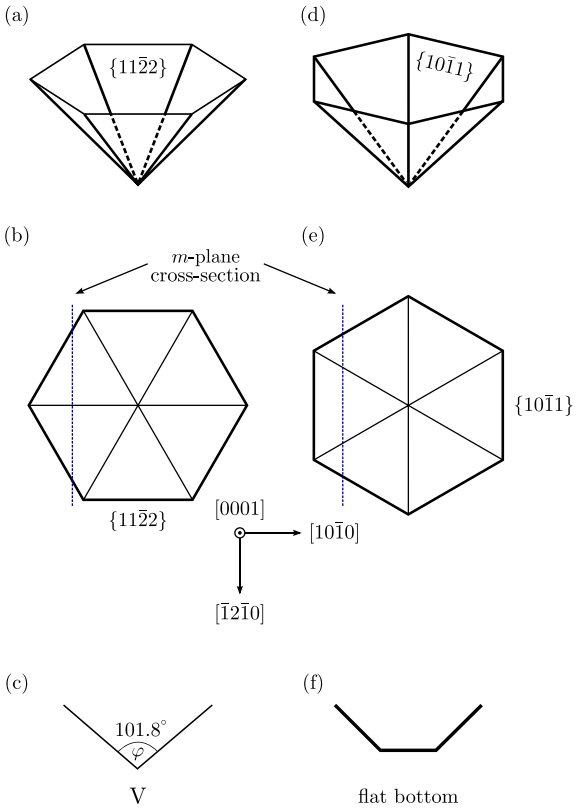

FIG. 2. Schematics of the three-dimensional structures (a,d), the top views (b,e), and cross sections at the m-plane (c,f) of hexagonal inverted pyramidal pits on a GaN wurtzite structure c-plane. (a–c) and (b–f) show a pit with (11$\bar{2}$2) and (10$\bar{1}$1) facets, exhibiting on the m cleavage plane a v-shaped profile or a profile with a flat bottom, respectively.

Hence, the inverted pyramids must consist of $\{11\bar{2}l\}$ facets. In order to determine l, we utilize the measured opening angle. This angle of 104° agrees well with $l = 2$, for which an opening angle of 101.8° is calculated. If a v-shaped defect is cleaved exactly through its center, the opening angle is reduced to 63.2°. However, due to the large size of the v-shaped defects it is much more likely to observe an off-center cleavage, where the opening angle on an m-plane cross section is 101.8°. Thus, the facets overgrown in these GaN epitaxial layers were $\{11\bar{2}2\}$ planes, which form the side facets of the inverted hexagonal pyramids as shown schematically in Fig. 2(a).

At this stage, we address the effect of overgrown v-defects on the electronic properties of the GaN epitaxial layers. For this purpose, we compare the tunneling properties far away from v-defects to spectra taken at the center of the v-defects cross section. In Fig. 1 there is no visible difference between the center and the areas away from the v-defects. Tunneling spectra also did not exhibit detectable differences. However, in other areas of the sample, the tunneling current becomes unstable near the cross-sectioned centers of the v-defects. This unstable tunneling behavior shows up as oscillations in the XSTM image (inset of Fig. 3). The region with oscillations is typically 1 to 3 μm wide and extending along c-direction.

The collapse of the tunneling current is only observable for positive voltages. At negative voltages, there are no

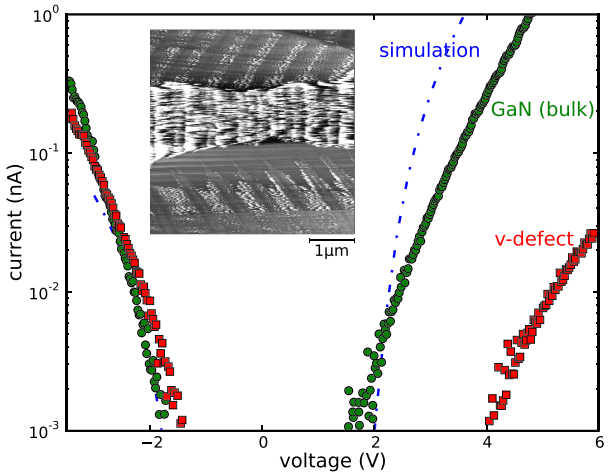

FIG. 3. Tunneling spectra at constant tip-sample separation measured at the center of a cross-sectioned v-shaped defect [(red) squares] and far away from the v-shaped defect [(green) circles]. The large apparent band gap of the tunneling spectrum at the v-shaped defect indicates a suppressed tunneling at positive voltages due to deep traps. The (blue) dashed-dotted line is a calculated spectrum assuming a pinning by surface defect states. It agrees well with the spectrum far away from the v-shaped defect. Inset: constant-current XSTM image with oscillations at the center of the v-shaped defect. The image shows the empty density of states acquired at a voltage of +4.0 V and 100 pA of set current.

significant changes in the tunneling current and the XSTM image does not shows oscillations. This behavior is corroborated and quantified by tunneling spectra acquired at the center and far away from the v-defects (Fig. 3). The spectra far away from the defects show an onset of the tunneling current of −1.8 V at negative voltages and an onset of +1.8 V at positive voltages. In contrast, spectra taken at the center of the v-defects exhibit a slightly smaller onset voltage at negative voltages, but a much larger onset voltage for the tunneling current at positive voltages of about +4.0 V. Hence, tunneling is significantly more difficult at positive voltages.

Simulations of the tunneling spectra[29] assuming a stepped *n*-type GaN surface pinned by the defect states, e.g., at step edges, and a band gap of 3.39 eV agree well with the measured tunneling spectra far away from the v-shaped defect [see (blue) dashed-dotted line in Fig. 3]. At positive voltages, the current arises from electrons injected into the conduction band. At negative voltages, the current is due to electrons extracted from the valence band states.[30] This agrees well with typical tunneling spectra taken on pinned *m*-plane cleavage surfaces of *n*-type GaN.[31,32] In contrast, the tunneling spectra taken in the vicinity of the center of the v-defect cannot be simulated with reasonable low carrier concentrations or material parameters as the apparent band gap widens strongly despite pinning. This indicates that the carrier dynamics within the GaN sample (not included in the calculation) inhibit an efficient injection of electrons.[33] It suggests the presence of deep electron traps at the center of the v-defect. Upon injection of an electron into the conduction band, it gets trapped by the deep trap and the surrounding GaN area charges up, inhibiting further electron tunneling. The deep traps cannot be emptied, as the concentration of holes in the valence band (minority carriers) is too low. However, when extracting electrons from the valence band at negative voltages, the presence of the deep traps does not affect the hole conductivity. Hence, a normal conductivity is observed at negative voltages, but not at positive ones, in agreement with the experimental observations.

At high positive voltages, at which a current is still observed, hot carriers are injected with energies significantly higher than the energy of the conduction band edge ($\gtrsim 2.5$ eV). Hot electrons require longer thermalization times during which they migrate over long distances, being able to leave the zone trapping of thermalized carriers.

At this stage, we discuss the spatial distribution of the deep traps. The fraction of v-shaped defects with deep traps (unstable tunneling conditions) is found to be about one third of the investigated length along the *c* direction. The transition between sections with stable tunnel current and sections without tunnel current, indicated by the oscillations, occurs along the same v-shaped defect without any evidence of the cross-sectional cleavage plane significantly being shifted with respect to the center of the v-shaped defect. Hence, the local absence of the tunneling current at positive voltages suggests that the deep traps are distributed inhomogeneously along the v-shaped defects. However, they are always located close to the imaged center of the cross-sectioned v-defect. Since we statistically cleave most of our cross sections somewhat off-center of the actual v-defect center, the observations of an inhomogeneous distribution of deep traps along the v-shaped defects may also be arising from fluctuating radial extensions of the distribution of deep traps along the v-shaped defects. The inhomogeneous electronic properties of the v-shaped defects observed in our XSTM investigation may explain the diverging reports about the electrical properties of v-shaped defects.[5,15–22]

In conclusion, we determined the geometric and electronic structure of overgrown v-shaped defects in GaN epitaxial layers by cross-section scanning tunneling microscopy and spectroscopy. The v-shaped defects were found to be hexagonal pit structures defined by six $\{11\bar{2}2\}$ planes. At their center, the v-shaped defects exhibit inhomogeneous electronic properties with areas where the tunneling current is inhibited. This indicates the presence of deep traps blocking the electron injection into overgrown v-shaped defects in the GaN epitaxial layer.

The authors thank the Deutsche Forschungsgemeinschaft for financial support under grant Nos. Eb197/5-1 and Ei788/2-1, K.-H. Graf for technical support, and V. Portz for help in the correction of the STM image distortion.

[1]S. Nakamura, Mater. Res. Soc. Bull. **34**, 101 (2009).
[2]Z. Lilienthal-Weber, Y. Chen, S. Ruvimov, and J. Washburn, Phys. Rev. Lett. **79**, 2835 (1997).
[3]Y. Chen, T. Takeuchi, H. Amano, I. Akasaki, N. Yamada, Y. Kaneko, and S. Y. Wang, Appl. Phys. Lett. **72**, 710 (1998).
[4]T. Paskova, E. M. Goldys, R. Yakimova, E. B. Svedberg, A. Henry, and B. Monemar, J. Cryst. Growth **208**, 18 (2000).
[5]X. H. Wu, C. R. Elsass, A. Abare, M. Mack, S. Keller, P. M. Petroff, S. P. DenBaars, J. S. Speck, and S. J. Rosner, Appl. Phys. Lett. **72**, 692 (1998).
[6]N. Sharma, P. Thomas, D. Tricker, and C. Humphreys, Appl. Phys. Lett. **77**, 1274 (2000).
[7]A. M. Sánchez, M. Gass, A. J. Papworth, P. J. Goodhew, P. Singh, P. Ruterana, H. K. Cho, R. J. Choi, and H. J. Lee, Thin Solid Films **479**, 316 (2005).

[8]M. C. Johnson, Z. Lilienthal-Weber, D. N. Zakhariv, D. E. McCready, R. J. Jorgenson, J. Wu, W. Shan, and E. D. Bourret-Courchesne, J. Electron. Mater. **34**, 605 (2005).
[9]H.-L. Tsai, T.-Y. Wang, J.-R. Yang, C.-C. Chuo, J.-T. Hsu, Z.-C. Feng, and M. Shiojiri, Mater. Trans. **48**, 894 (2007).
[10]J.-R. Yang, W.-C. Li, H.-L. Tsai, J.-T. Hsu, and M. Shiojiri, J. Microsc. **237**, 275 (2010).
[11]L. Zhou, M. R. McCartney, D. J. Smith, A. Mouti, E. Feltin, J. F. Carlin, and N. Grandjean, Appl. Phys. Lett. **97**, 161902 (2010).
[12]B. Pécz, Z. Makkai, M. A. di Forte-Poisson, F. Huet, and R. E. Dunin-Borkowski, Appl. Phys. Lett. **78**, 1529 (2001).
[13]A. Hangleiter, F. Hitzel, C. Netzel, D. Fuhrmann, U. Rossow, G. Ade, and P. Hinze, Phys. Rev. Lett. **95**, 127402 (2005).
[14]S. Tomiya, Y. Kanitani, S. Tanaka, T. Ohkubo, and K. Hono, Appl. Phys. Lett. **98**, 181904 (2011).
[15]T. Paskova, E. M. Goldys, and B. Monemar, J. Cryst. Growth **203**, 1 (1999).
[16]T. Riemann, J. Christen, B. Beaumont, J.-P. Faurie, and P. Gibart, Superlattices Microstruct. **36**, 833 (2004).
[17]W. Lee, H. J. Lee, S. H. Park, K. Watanabe, K. Kumagai, T. Yao, J. H. Chang, and T. Sekiguchi, J. Cryst. Growth **351**, 83 (2012).
[18]J. Elsner, R. Jones, M. Haugk, R. Gutierrez, T. Frauenheim, M. I. Heggie, S. Öberg, and P. Briddon, Appl. Phys. Lett. **73**, 3530 (1998).
[19]A. Lochthofen, W. Mertin, G. Bacher, L. Hoeppel, S. Bader, J. Off, and B. Hahn, Appl. Phys. Lett. **93**, 022107 (2008).
[20]L. C. Le, D. G. Zhao, D. S. Jiang, L. Li, L. L. Wu, P. Chen, Z. S. Liu, Z. C. Li, Y. M. Fan, J. J. Zhu, H. Wang, S. M. Zhang, and H. Yang, Appl. Phys. Lett. **101**, 252110 (2012).
[21]M. Herrera, A. Cremades, M. Stutzmann, and J. Piqueras, Superlattices Microstruct. **45**, 435 (2009).
[22]C. L. Progl, C. M. Parish, J. P. Vitarelli, and P. E. Russell, Appl. Phys. Lett. **92**, 242103 (2008).
[23]H. Eisele, L. Ivanova, S. Borisova, M. Dähne, M. Winkelnkemper, and Ph. Ebert, Appl. Phys. Lett. **94**, 162110 (2009).
[24]H. Eisele and Ph. Ebert, Phys. Status Solidi (RRL) **6**, 359 (2012).
[25]Ph. Ebert, L. Ivanova, S. Borisova, H. Eisele, A. Laubsch, and M. Dähne, Appl. Phys. Lett. **94**, 062104 (2009).
[26]M. Schnedler, P. Weidlich, V. Portz, D. Weber, R. Dunin-Borkowski, and Ph. Ebert, "Correction of nonlinear lateral distortions of scanning probe microscope images" (unpublished).
[27]Z. Liliental-Weber, M. Benamara, W. Swider, J. Washburn, I. Grzegory, S. Porowski, R. D. Dupuis, and C. J. Eiting, Physica B **273–274**, 124 (1999).
[28]E. Richter, U. Zeimer, S. Hagedorn, M. Wagner, F. Brunner, M. Weyers, and G. Tränkle, J. Cryst. Growth **312**, 2537 (2010).
[29]R. M. Feenstra, J. Vac. Sci. Technol. B **21**, 2080 (2003); R. M. Feenstra, S. Gaan, G. Meyer, and K. H. Rieder, Phys. Rev. B **71**, 125316 (2005); R. M. Feenstra, Y. Dong, M. P. Semtsiv, and W. T. Masselink, Nanotechnology **18**, 044015 (2007); Y. Dong, R. M. Feenstra, M. P. Semtsiv, and W. T. Masselink, J. Appl. Phys. **103**, 073704 (2008); N. Ishida, K. Sueoka, and R. M. Feenstra, Phys. Rev. B **80**, 075320 (2009); S. Gaan, G. He, R. M. Feenstra, J. Walker, and E. Towe, J. Appl. Phys. **108**, 114315 (2010); R. Feenstra, SEMITIP version 6, 2011.
[30]Ph. Ebert, L. Ivanova, and H. Eisele, Phys. Rev. B **80**, 085316 (2009).
[31]L. Ivanova, S. Borisova, H. Eisele, M. Dähne, A. Laubsch, and Ph. Ebert, Appl. Phys. Lett. **93**, 192110 (2008).
[32]M. Bertelli, P. Löptien, M. Wenderoth, A. Rizzi, R. Ulbricht, M. Righi, A. Ferretti, L. Martin-Samos, C. Bertoni, and A. Catellani, Phys. Rev. B **80**, 115324 (2009).
[33]N. Jäger, E. Weber, K. Urban, and Ph. Ebert, Phys. Rev. B **67**, 165327 (2003).